MOL #16741

# Drug binding interactions in the inner cavity of hERG: Molecular insights from structure-activity relationships of clofilium and ibutilide analogues.

Matthew Perry, Phillip J. Stansfeld, Joanne Leaney, Claire Wood, Marcel J. de Groot, Derek Leishman

, Michael J. Sutcliffe and John S. Mitcheson.


Primary laboratory of origin:
MP and JSM
Department of Cell Physiology and Pharmacology,
Maurice Shock Medical Sciences Building,
University of Leicester,
University Road,
Leicester,
LE1 9HN,
United Kingdom.

JL, CW, MJG, DL.
Pfizer Global Research & Development,
Pfizer Limited,
Ramsgate Road,
Sandwich,
Kent,
CT13 9NJ,
United Kingdom.

PJS and MJS.
Department of Biochemistry,
Adrian Building,
University of Leicester,
University Road,
Leicester,
LE1 7RH,
United Kingdom.

1

MOL #16741

**Running title: Drug binding interactions in the inner cavity of hERG.**

Address correspondence to:
John Mitcheson
University of Leicester,
Department of Cell Physiology and Pharmacology,
Maurice Shock Medical Sciences Building,
University Road,
Leicester,
LE1 9HN,
United Kingdom.
Telephone: +44 (0)116 229 7133
Fax: +44 (0)116 252 5045
E-mail: jm109@le.ac.uk

Text pages = 32
Tables = 3
Figures = 8
References = 39
Words in abstract = 245
Words in introduction = 772
Words in discussion = 1845

Non-standard abbreviations:
hERG: human *ether a go-go* related gene
MK-499: (+)-*N*-[1′-(6-cyano-1,2,3,4-tetrahydro-2(R)-naphthalenyl)-3,4-dihydro-4(*R*)-hydroxyspiro(2*H*-1-benzopyran-2,4′-piperidin)-6-yl]methanesulfonamide] monohydrochloride.
E-4031: 1-[2-(6-methyl-2-pyridyl)ethyl]-4-(methylsulfonyl-aminobenzoyl)piperidine.
S6: sixth transmembrane segment.
MES: 2-[*N*-morpholino]ethanesulfonic acid.
Clofilium: 4-chloro-*N*,*N*-diethyl-*N*-heptylbenzenebutanaminium.
ClogP: Calculated logarithm of partitioning coefficient.

## Abstract

Block of hERG $K^+$ channels by otherwise useful drugs is the most common cause of long QT syndrome, a disorder of cardiac repolarization that predisposes patients to potentially fatal arrhythmias. This undesirable LQT side effect has been a major reason for the withdrawal of medications from the pharmaceutical market. Understanding the molecular basis of hERG block is therefore essential to facilitate the design of safe drugs. Binding sites for hERG blockers have been mapped within the inner cavity of the channel and include aromatic residues in the S6 helix (Tyr-652, Phe-656) and residues in the pore helix (Thr-623, Ser-624, Val-625). We use mutagenesis of these residues, combined with an investigation of hERG block by close analogues of clofilium and ibutilide, to assess how specific alterations in drug structure impact on potency and binding interactions. While changing the basic nitrogen from quaternary to tertiary accelerated the onset of block, the $IC_{50}$ and kinetics for recovery from block were similar. In contrast, analogues with different para-substituents on the phenyl ring had significantly different potencies for wild-type hERG block. The highest potency was achieved with polar or electronegative para-substituents, while neutral para-substituents had potencies more than 100-fold lower. Results from mutagenesis and molecular modelling studies suggest phenyl ring para-substituents influence drug interactions with Thr-623, Ser-624 and Tyr-652 and strongly impact binding affinity. Together, these findings suggest that modifying the para-substituent could be a useful strategy for reducing hERG potency and increasing the safety margin of compounds in development.

3

## Introduction

hERG (human ether-a-go-go related gene) potassium ($K^+$) channels mediate the rapidly activating delayed rectifier $K^+$ current ($I_{Kr}$) (Sanguinetti *et al*., 1995) that plays a key role in repolarization of the ventricular action potential (Tseng 2001, Vandenberg *et al*., 2001). Block of hERG by a wide variety of medications is linked to acquired long QT syndrome, a disorder characterised by lengthening of ventricular action potential duration (represented by an extension of the QT interval on an electrocardiogram), and an increased risk of ventricular arrhythmias and sudden death (Keating & Sanguinetti, 2001). The potential of a drug to cause QT prolongation has been a commonly cited reason for the withdrawal of medications from the pharmaceutical market. As a result, compounds are now subjected to time consuming and expensive screening procedures during development (Fermini & Fossa, 2003; Recanatini et al., 2004). An accurate understanding of the molecular basis of drug binding to hERG would significantly facilitate the development and safety profile of new medications (Sanguinetti and Mitcheson, 2005).

Block of hERG $K^+$ channels by most drugs requires opening of the activation gate, indicating that compounds bind within the inner cavity (Spector *et al*., 1996; Mitcheson *et al*., 2000a). Available evidence suggests hERG has a relatively large inner cavity compared to the $K_V$ channel family (Mitcheson *et al*., 2000a; Mitcheson & Perry, 2003). Previous studies have used mutagenesis to identify the amino acid residues lining the inner cavity of hERG that are essential for high-affinity block (Lees-Miller *et al*., 2000; Mitcheson *et al*., 2000b). Two aromatic residues on the inner (S6) helix (Tyr-652 and Phe-656), that are unique to the EAG $K^+$ channel family, are critical for binding of most hERG channel blockers (Mitcheson *et al*., 2000b; Kamiya *et al*., 2001; Sánchez-Chapula *et al*., 2002, 2003). Fluvoxamine and dronedarone are examples of drugs in which neither aromatic residue is critical for block (Ridley *et al*., 2004; Milnes *et al*., 2003). Nevertheless, most compounds interact with one or both. Mutagenesis studies suggest an aromatic residue is required at position 652 for high affinity binding with drugs through either cation-$\pi$ or $\pi$-stacking interactions with charged nitrogen and aromatic groups (Fernandez *et al*., 2004). In contrast, potency correlates well with hydrophobic indices of residues substituted into position 656 (Fernandez *et al*., 2004). Gating-dependent positioning of these residues

4

relative to the inner cavity (particularly with inactivation) may be critical for high-affinity binding (Chen *et al.*, 2002) and could explain the higher potency of compounds for hERG compared to EAG block (Herzberg 1998, Ficker 2001).

Three residues at the base of the pore helix (Thr-623, Ser-624 and Val-625), immediately adjacent to the GFG signature sequence of the selectivity filter, have been implicated as potential binding sites for some high-affinity compounds (Mitcheson *et al.*, 2000b; Perry *et al.*, 2004). All three residues are highly conserved in voltage-gated $K^+$ channels (Shealy *et al.*, 2003). However, their contribution to drug binding (as indicated by shifts in potency with alanine substitutions) is variable when comparing compounds of relatively similar structure (Mitcheson *et al.*, 2000b; Perry *et al.*, 2004). For example, ibutilide and clofilium have few differences in structure and similar potencies for wild-type (WT) hERG block. Nevertheless, marked differences exist in the kinetics of recovery from block and in their sensitivity to mutation of pore helix residues (Perry *et al.*, 2004). Specifically, the fold change in $IC_{50}$ caused by the S624A mutation was much higher for clofilium (381-fold) than for ibutilide (50-fold). Furthermore, the unusually slow recovery from clofilium block observed with WT and most mutant hERG channels was accelerated by the mutation S624A. These results suggested that clofilium formed a specific interaction with Ser-624 and illustrates the importance of pore helix residues for drug binding.

In this study, we used a range of closely related structural analogues of clofilium and ibutilide to investigate the molecular basis for the observed differences in hERG block. Clofilium and ibutilide differ in three ways. (1) The basic nitrogen atom is quaternary in clofilium but tertiary in ibutilide. (2) Ibutilide, but not clofilium, contains a benzylic hydroxyl group on the phenyl-amine linker. (3) The para-substituent on the phenyl ring is a chlorine in clofilium and a methanesulfonamide in ibutilide. We demonstrate that the quaternary nitrogen on clofilium confers slow onset of block kinetics. The $IC_{50}$ of the tertiary analogue is similar to clofilium. This probably arises because, although membrane permeability of the tertiary analogue is higher than that of clofilium, mutagenesis studies suggest the inner cavity binding affinity is lower. Remarkably, drug potency was reduced 100-fold by alterations to the para-substituent. Mutagenesis and molecular modelling studies suggest this is due to less favourable interactions with Thr-623, Ser-624 and Tyr-652.

5

## Materials and Methods:

### hERG mutagenesis and expression in Oocytes.

hERG channel mutations were introduced by site-directed mutagenesis (Quikchange, Stratagene), subcloned into the pSP64 expression vector and confirmed by DNA sequencing. Complementary RNA for WT and mutant hERG channel expression in *Xenopus laevis* oocytes was prepared by *in vitro* transcription using SP6 RNA polymerase (mMessage mMachine kit, Ambion) after linearization of the hERG construct with EcoR1. De-folliculated oocytes were maintained in culture and injected with cRNA as described previously (Sanguinetti & Xu, 1999).

### Voltage clamp recordings.

The two-microelectrode voltage clamp technique was used to record membrane ionic currents from WT or mutant hERG channels between 1 and 7 days after injection. Currents were recorded, at room temperature, with a GeneClamp 500B amplifier, digitized at 5 kHz with a Digidata 1322A (Axon Instruments, Inc., Union City, CA) and saved to computer for off-line analysis. Data acquisition and analysis were performed using pClamp8.2 software (Axon Instruments), and further analysis performed using Prism 4.01 software (GraphPad Software, San Diego, CA). Endogenous chloride currents were attenuated by using a low-chloride extracellular recording solution in which chloride was replaced with 2-[*N*-morpholino]ethanesulfonic acid (MES). The extracellular solution contained: 96 mM NaMES, 2 mM KMES, 2 mM CaMES$_2$, 5 mM HEPES, and 1 mM MgCl$_2$, pH adjusted to 7.6 with NaOH. To record currents from hERG channel mutants that exhibit a left shift in the voltage-dependence of inactivation (T623A and T623A:S624A), a high-K$^+$ extracellular solution containing 96 mM KMES and 2 mM NaMES (with all other constituents the same) was used (Mitcheson *et al*. 2000b). Extracellular solutions were applied from a solution-switching device that allowed the solution outlet barrel to be placed adjacent to the oocyte, directing solution flow around the oocyte (Mitcheson *et al*., 2000a). This, together with the high flow rate (3 to 4 mlmin$^{-1}$), minimised extracellular K$^+$ accumulation and allowed solution changes in less than 10-s. Microelectrodes were pulled from borosilicate glass using a horizontal micropipette puller (Sutter Instruments), filled with 3M KCl and tips broken to give resistances of 1 to 2 MΩ.

6

**Protocols and Pharmacology.**

Clofilium (4-chloro-$N$,$N$-diethyl-$N$-heptylbenzenebutanaminium) tosylate was purchased from Alexis Corp, UK. The clofilium analogues were supplied by Pfizer UK. All compounds were dissolved in dimethyl sulfoxide to produce 10 mM stocks and stored at -20°C. On the day of the experiment, drug stocks were diluted to the required concentration in the appropriate extracellular solution. Unless otherwise stated, the protocol used to assess hERG drug block was performed by applying a 5 s depolarizing pulse from a holding potential of –90 mV to 0 mV before measuring peak tail current amplitude upon repolarization to –70 mV for 400 ms. Prior to drug application, oocytes were repetitively depolarized every 6 s until current amplitudes were stable over 10 pulses. Repetitive depolarizing pulses were then applied in the presence of drug until steady-state block was reached. This protocol ensures the channels are in the open-inactivated conformation for the majority of the time. Leak subtraction was performed by stepping briefly to –70 mV from the holding potential and subtracting the resulting leak current from the peak hERG channel tail currents. Currents following drug addition were normalised to control ($I_{Drug}/I_{Control}$). The concentration of drug that achieved half-maximal inhibition ($IC_{50}$) was obtained by fitting data with a Hill function,

$$I_{Drug}/I_{control} = 1 / (1 + ([D] / IC_{50})^h) \qquad \text{Equation 1}$$

in which [D] and $h$ correspond to the drug concentration and Hill coefficient respectively.

Current-voltage ($I$-$V$) relationships were generated by applying 5 s depolarizing pulses from a holding potential of –90 mV, to potentials between –60 mV and +50 mV in 10 mV increments, with tail currents measured at –70 mV. The half-point ($V_{0.5}$) and slope factor (k) for the voltage dependence of activation were obtained by fitting peak tail current-voltage relationships with a Boltzmann function. Current reversal potential and deactivation kinetics were determined from tail currents at potentials between +30 mV and –140 mV following 1 s depolarization to +30 mV to fully activate hERG currents. Time constants for deactivation were obtained by fitting tail current decay with exponential functions. Data are presented as mean ± S.E.M., and $n$ refers to the number of oocytes. Statistical analysis to compare biophysical properties and blocking potency of mutant to

7

wild-type hERG channels were performed using either ANOVA tests with Dunnet's comparison or students t-test (as indicated). Differences were considered significant for $P < 0.05$.

**Homology modelling.**

An homology model of hERG was created using Modeller 6 (Sali & Blundell, 1993), with KcsA [PDB (Berman *et al.*, 2000) code 1bl8; Doyle *et al.*, 1998] as the template structure. Ten homology models were generated, with the lowest energy model selected. To eliminate the effects of residues Ser-649 and Ser-660 – as mutagenesis appears to preclude their involvement in drug binding (Perry *et al*., 2004) – the S6 transmembrane helices of the model were rotated slightly, using the Yale Morph Server (http://www.molmovdb.org/morph/), so that these two serine residues are displaced from the binding site – thus preventing them from influencing ligand binding - while the aromatic residues remain exposed to the binding site. This approach will be described in detail elsewhere (Stansfeld, Gedeck, Mitcheson & Sutcliffe – Drug block of the hERG potassium channel: insight from modeling – manuscript in preparation). Sybyl6.8 (Tripos Inc., St Louis, MO, USA) was used to build the ligand structures. Drug dockings were performed using GOLD (Jones *et al*., 1997), without restraints; using a sphere radius of 20, with an origin central to the cavity. The ligand dockings were scored based on the parameters of the GoldScore function, with the top ten binding modes retained. hERG-ligand complexes were visualised using Pymol (DeLano, 2002).

## Results

**Camparison of quaternary clofilium with a tertiary analogue**

Ibutilide and clofilium are ammonium salts that share similar core structures consisting of a phenyl ring, a four-carbon linker to a central nitrogen, and a seven-carbon aliphatic tail. Despite having a similar potency they exhibit different recovery from block kinetics and binding site interactions within the inner cavity of hERG (Perry *et al*., 2004). One potentially important structural difference between these two compounds is that clofilium is a quaternary ammonium salt whereas ibutilide is a tertiary compound. The tertiary central nitrogen on ibutilide allows the compound to exist in a neutral or protonated (positively charged) state at physiological pH. By contrast, the quaternary central nitrogen on clofilium carries permanent positive charge that confers low lipid permeability and is thought to be responsible for its slow equilibration across the plasma membrane and slow kinetics for hERG block (Castle 1991; Gessner & Heinemann, 2003). To determine if the extra ethyl group on the central nitrogen (and permanent positive charge) is responsible for the distinct kinetics and/or binding of clofilium, we compared block by a tertiary analogue PNU-0068611A (structures given in Figure 1A).

Representative WT-hERG current traces before (control) and after steady-state block by clofilium (i) and PNU-0068611A (ii) are shown in Figure 1B. Both compounds blocked WT-hERG with similar high-affinity (Figure 1C). The $IC_{50}$ of PNU-0068611A was $80.84 \pm 20.8$nM (n=4) (Figure 1C), which compares with an estimated $IC_{50}$ of 30nM for clofilium (Perry *et al*., 2004). As previously discussed (Perry et al, 2004), the $IC_{50}$ for clofilium is difficult to precisely measure because of the extraordinary slow time course for onset of block with low (< 100 nM) concentrations (Gessner & Heinemann, 2001; Perry *et al*., 2004). Percentage block with 300 nM was slightly greater for the quaternary than tertiary compound. There were, however, very significant differences in the rates of onset of block. Steady-state block by PNU-0068611A occurred within a single pulse (Figure 1D). Fitting with a single exponential function produced mean time constants for the onset of block with 10μM of $2.14 \pm 0.37$s (n=4) and $23.11 \pm 0.46$s (n=4) for PNU-0068611A and clofilium respectively (P < 0.005, unpaired *t*-test). These findings clearly demonstrate that the permanent positive charge of clofilium is responsible for the slow onset kinetics. Other tertiary analogues of cloflium (see later), without the benzylic

9

hydroxyl group of PNU-0068611A, also exhibit rapid block, suggesting the hydroxyl group does not contribute significantly to the kinetics of block by PNU-0068611A.

Alanine scanning mutagenesis has previously been used to identify several residues at the base of the pore helices (Thr-623, Ser-624, Val-625) and on S6 helices (Gly-648, Tyr-652, Phe-656, Val-659) that are required for high affinity block by ibutilide and clofilium (Perry *et al.*, 2004). However, the increase in $IC_{50}$ (representative of decreased affinity) with each alanine mutation varied between the two compounds, suggesting different binding conformations. To examine whether the quaternary amine of clofilium mediated these effects we compared block of pore helix and S6 helix mutants by clofilium and the tertiary analogue PNU-0068611A. A positive shift in the voltage dependence of activation or dramatic slowing of deactivation can contribute to a decrease in sensitivity to drug block. The mean slope (k), half-maximal point of activation ($V_{0.5}$) and time constants for deactivation of WT and mutant hERG channels are given in Table 1. Only the S624T mutation produced a significant shift in $V_{0.5}$ of activation compared to WT-hERG (-17.3 ± 0.8 mV for S624T vs. –22.4 ± 1.6mV for WT-hERG, P < 0.01 one-way ANOVA-test). S624A time constants of deactivation were statistically significantly slower (P < 0.05) than WT. However, neither change is likely to be sufficient to significantly alter sensitivity to block.

To investigate the relative importance of pore helix residues in drug binding and to test if interactions with the quaternary amine are required for clofilium block, tertiary analogues and clofilum were applied to alanine mutants and the effects on $IC_{50}$ measured relative to WT hERG. Figure 2A shows typical S624T (i) and S624A (ii) hERG currents before (control) and during exposure to increasing concentrations of PNU-0068611A. All pore helix mutant channels exhibited decreased sensitivity to block by both compounds (Figure 4B). The rank order of importance for mutations that decrease binding affinity was T623A:S624A> V625A> S624A> S624T> T623A for PNU-0068611A and T623A:S624A> S624A> V625A> S624T> T623A for clofilium. For both compounds, the greatest fold shift in $IC_{50}$ was observed with the double T623A:S624A mutation, with smaller shifts for the single mutants (Figure 2C). Therefore, substitution of either polar residue may, to some extent, be compensated for through binding to the remaining polar residue. Both analogues have a greater affinity for Ser-624 than with Thr-623, suggesting the spatial positioning of the hydroxyl group of Ser-624 is

more optimal than with Thr-623. Indeed, the conserved mutation S624T reduced, but did not abolish, the loss of sensitivity to block observed with the S624A mutation, indicating the importance of appropriate positioning of the hydroxyl group. Interestingly, high concentrations of clofilium and the tertiary analogue caused an apparent slowing of S624T hERG deactivation (Figure 2A). This phenomenon probably due to recovery from block upon repolarisation, was not observed in S624A or other mutant channels and suggests a reduction of binding affinity upon channel deactivation. A transient component of current due to the re-onset of block can be seen at the beginning of the test pulses (Figure 2Ai).

Very slow recovery from block is a feature of clofilium (Figure 5A) and is likely to contribute to its high potency. Clofilium recovery from block is much slower than ibutilide and we have previously shown that this is due to differences in binding interactions rather than drug trapping (Perry *et al.*, 2004). To test if the quarternary amine group is required, we investigated recovery from block of the tertiary clofilium analogue. WT-hERG current was inhibited by >95% by 10 $\mu$M PNU-0068611A. Following removal of drug from the recording solution and with continuous repetitive pulsing to 0mV for 20 minutes only minimal (< 5 %) recovery from block was observed (Figure 3C), similar to clofilium. Thus the quaternary amine is not responsible for this property. In contrast, recovery from block of S624A hERG by PNU-0068611A and clofilium was rapid (Figure 3C). Mean values for recovery from block after 20 minutes, expressed as a percentage of initial steady-state block, were $99.6 \pm 0.2\%$ and $78.4 \pm 6.5\%$ for clofilium and PNU-0068611A respectively (Figure 3D). Thus, the slow recovery from block is dependent on Ser-624, and does not require the quaternary amine of clofilium.

Both PNU-0068611A and clofilium exhibited a similar pattern of shifts in $IC_{50}$ for the pore helix mutants, suggesting they share the same binding sites on this region of the channel. However, the size of the shifts in $IC_{50}$ for all pore helix mutants was much greater for the quaternary compound (see Figure 2C) suggesting more favourable interaction energies compared to the tertiary analogue. For S6 mutants (Y652A and F656A) the pattern was different (Figure 4). While F656A shifted $IC_{50}$ for both compounds by similar amounts (484- and 420-fold for clofilium and PNU-0068611A, respectively), the shifts were markedly different for Y652A (1329-fold for clofilium and 193-fold for PNU-0068611A). These findings indicate a stronger interaction with Tyr-652 for clofilium than PNU-0068611A, for which there are several possible explanations.

11

First, the addition of a hydroxyl group one carbon from the phenyl ring on PNU-0068611A may alter its electrostatic potential and decrease the affinity of the π-stacking interaction with Tyr-652. Second, the removal of an ethyl group from the central nitrogen would remove its permanent positive charge and decrease the affinity of the cation-π interaction with Tyr-652. However, this seems unlikely given the predicted $pK_a$ is 9.96 and therefore >99% of PNU-0068611A molecules are predicted to be protonated. Alternatively, removal of an ethyl group may reduce hydrophobic interactions with Tyr-652 – as suggested by our docking studies. Third, removal of an ethyl group and/or the addition of the hydroxyl group may allosterically alter the positioning of the compound within the inner cavity thereby decreasing its ability to interact at one or more binding sites. Some evidence for this comes from a 3-D QSAR (quantitative structure activity relationship) pharmacophore study in which a decrease in volume around the lower region of the phenyl ring (equivalent to loss of hydroxyl group) or an increase in volume around the central nitrogen (equivalent to the addition of an ethyl group) increased pharmacophore activity (Cavalli *et al*., 2002). The increased interaction of clofilium with Tyr-652 would presumably also stabilize the drug to enable optimum interactions of the para-substituent with pore helix residues.

*Effect of changing the para-substituent on the phenyl ring*

Another important difference between ibutilide and clofilium is in the nature of the para-substituent attached to the phenyl ring, which is a methanesulfonamide in ibutilide and chlorine in clofilium (see Figure 1A). Mutagenesis and modeling data so far suggests that the para-substituent interacts with polar residues (Thr-623 and Ser-624) at the base of the pore helix (Perry *et al*., 2004). If this is the case then specific changes in the nature of the para-substituent would be expected to alter compound potency and influence the relative shifts of $IC_{50}$ caused by pore helix mutations. To test this hypothesis we compared PNU-0068611A with three analogues in which nitro, amine or amide groups replaced the chlorine (structures shown in Figure 5A-C). In WT-hERG $IC_{50}$ values varied by more than 100-fold. The rank order of potency was nitro> chlorine> amine> amide, with $IC_{50}$ concentrations of 2.51 ± 0.4nM (n=5), 80.8 ± 20.8nM (n=4), 273.2 ± 16.8nM and 328.7 ± 91.2nM, respectively. Clearly, the identity of the para-substituent has dramatic affects on potency. This is not only a

feature of clofilium analogues. Altering the para-substituents of dofetilide (Table 2) also impacts on potency. Thus, despite UK-068522 and UK-068097 having identical core structures (i.e. the same central nitrogen, linkers and number of cyclic carbon rings), differences in the para-substituents resulted in these compounds being 54- and 20-fold less potent than dofetilide.

To investigate the reason for the dependency of compound potency on the nature of the para-substituent, we determined the sensitivity of different substituents to mutations of pore (Thr-623, Ser-624 & Val-625) and S6 (Tyr-652 & Phe-656) helix residues (Figure 6A and B). The fold change in potency induced by the double mutant T623A:S624A was greatest in the nitro compound and decreased as compound potency to WT-hERG decreased (Figure 6C). This further implicates two polar pore helix residues (Thr-623 and Ser-624) as sites of interaction with para-substituents of compounds and suggests that the differences in block by ibutilide and clofilium are due to properties of the para-substituent. Further mutational analysis of pore helix interactions was not possible because mutations were not tolerated. We were unable to obtain functional expression of Val, Leu, Ile, Cys, Lys, Tyr and Asn mutants at positions 623 and 624. With the exception of V625A, mutations of Val-625 were also non-functional. In $K^+$ channels these residues are highly conserved (Shealy *et al.*, 2003) and being so close to the selectivity filter are clearly important for channel function.

Mutation of S6 helix residues Tyr-652 and Phe-656 to Ala greatly reduced sensitivity to block by all four para-substituent analogues (Table 3). The fold reduction in potency was similar for chlorine, amine and amide analogues on both Y652A (129- to 193-fold) and F656A (420- to 422-fold) hERG channels. However, much larger shifts in $IC_{50}$ were observed with the nitro- compound on Y652A (1833-fold) and F656A (2688-fold) hERG channels. Therefore, the most potent compound for WT-hERG block (at least 20-fold more potent than the chlorine containing compound) also exhibited the greatest decrease in potency with Y652A and F656A (Figure 6D).

The relationship between the potency of each compound and the fold shift in $IC_{50}$ induced by alanine mutations of the pore and S6 helix residues is shown in Figure 7. Good correlation exists between potency on WT-hERG and fold-shifts induced by T623A:S624A and Y652A, suggesting that interactions with these residues play a particularly important role in high-affinity binding.

13

Discussion

**Permanent positive charge on clofilium confers slow kinetics of block, without affecting recovery from block or hERG binding site interactions.**

Ultra-slow kinetics for the onset of $K^+$ channel block by quaternary clofilium has previously been reported in *Xenopus* oocytes (Suessbrich *et al.*, 1997; Steidl & Yool, 2001; Perry *et al.*, 2004), mammalian cell lines (Gessner & Heinemann, 2003) and rat ventricular myocytes (Castle, 1991). As predicted, the slow kinetics of block were not observed with the tertiary clofilium compound PNU-0068611A, which differs from clofilium only in the removal of an ethyl group from the central quaternary nitrogen and the addition of a benzylic hydroxyl group (Figure 1). The hydroxyl is unlikely to contribute to the rapid onset of block since similar rapid kinetics were observed with other tertiary clofilium analogues in which it is absent. Slow equilibrium across the membrane due to the permanent positive charge of clofilium is most likely responsible for the slow onset of block.

Clofilium and PNU-0068611A differ only two-fold in their potency for WT-hERG block. However, the potency of extracellularly applied quaternary clofilium is most likely an underestimation of binding affinity due to slow and incomplete equilibration across the membrane in the whole cell configuration. Indeed, clofilium block of hEAG1 channels is faster and the $IC_{50}$ much lower, when applied to intracellular side of channels in excised patches (Gessner & Heinemann, 2003). Thus, it is likely that clofilium has a significantly higher potency for WT-hERG block than the tertiary compound. Unfortunately, hERG current rundown from excised inside-out patches is too rapid to determine the $IC_{50}$ of drugs applied to the intracellular side of channels (personal observation; also conclusion of Gessner and Heinemann, 2003). Our mutagenesis results indicate that both compounds share the same binding sites on hERG but shifts in $IC_{50}$ were much greater for clofilium. Thus, small changes in compound structure – such as the addition of an ethyl group or removal of a hydroxyl group – can optimise inner cavity binding site interactions, and thereby increase potency.

Slow recovery from clofilium block is not due to a protonated, charged amine group since the tertiary compound unbinds with a similar slow rate to clofilium. Thus, in contrast to classical experiments on block of

14

sodium channels by anaesthetics (Hille et al., 1977; Hondeghem & Katzung, 1977), there is no evidence of hydrophilic pathways through which uncharged drug molecules could escape from the inner cavity of hERG.

**Para-substituents interact with pore helix residues.**

A large number of structurally diverse compounds have a high affinity for hERG. Structural features that are common to many are one or more phenyl rings and a charged central nitrogen 5.2 to 9.1 Å apart separated by a carbon atom linker (Cavalli *et al*., 2002; Ekins *et al*., 2002; Pearlstein *et al*., 2003). In this study, we show that the para-substituent on the phenyl ring of clofilium can also substantially influence drug potency. There was more than a 100-fold shift in $IC_{50}$ in the limited range of analogues we studied. Of the four tertiary analogues we tested, the rank order of potency against WT-hERG upon modifying the para-substituents was nitro> chlorine> amine> amide. Therefore, analogues with polar or electronegative para-substitunts are more potent than those with neutral moieties. Similar results were obtained using a range of dofetilide analogues (Table 2), indicating these findings were not restricted to clofilium analogues. Interestingly, Cavalli *et al*. (2002) highlighted polar (e.g. methanesulfonamides or nitro moieties) or polarizable (halogen atoms such as chlorine) regions in close proximity to the primary phenyl ring in their 3D-QSAR model of hERG channel blockers. It is possible that modifying the nature of the para-substituent could be a viable strategy for reducing hERG potency and liability to cause QT prolongation.

Of the hERG channel mutations tested, a good correlation between fold change in $IC_{50}$ and potency of para-substituent analogues for WT-hERG block was obtained with the double mutant T623A:S624A. In fact, this mutant shifted (weakened) the $IC_{50}$ of the nitro- analogue by approximately 1000-fold, indicating the importance of these residues for drug interactions. Therefore, we propose that the increased potency of compounds with polar para-substituents is due to an enhanced affinity with the polar residues (Thr-623 and Ser-624) that face the inner cavity of hERG from the base of the pore helix. In addition, mutation of Tyr-652 (but not Phe-656) on the S6 helix, also showed good correlation suggesting that a combination of these two sites are important for high-affinity block.

*In silico* **modelling**

15

The hERG-ligand complexes produced by our docking studies appear to be consistent with the experimental results, thus aiding interpretation of the data at the atomic level. The apparent optimal binding mode for the ligand structures – adopted by all but ibutilide and the amide analogue – is illustrated by the nitro analogue in Figure 8. In this mode, the para-substituent interacts with both Thr-623 and Ser-624 in the top corner of the cavity, while the phenyl ring is located where it may form a weak π-stacking interaction with the aromatic ring of Tyr-652. Interestingly, in accordance with a previous report (Perry *et al*., 2004), this binding mode – in particular access to the top corner of the cavity – would be impeded by the additional methyl group of the G648A mutant. Additionally, the protonated central nitrogen sits central to the cavity, roughly 5Å from all four Tyr-652 aromatic rings, with which it is predicted to form cation-π interactions. Consistent with these findings, mutating Tyr-652 to a range of amino acids indicated that the aromaticity of the residue in this position is important for high-affinity block (Fernandez *et al*., 2004). The ethyl groups attached to the central nitrogen may also form hydrophobic interactions with Tyr-652. The second ethyl group of clofilium may contribute an additional hydrophobic interaction with one of the Y652 sidechains, making it more sensitive to the Y652A mutation than the tertiary analogue.

Ser-624, located at the C-terminal end of the pore helix, is an important site of interaction with clofilium. Mutation of Ser-624 to Ala substantially reduced hERG block and facilitated recovery from block. However, S624A caused much smaller shifts in $IC_{50}$ compared to the T623A:S624A double mutation. Our model predicts that despite their close spatial proximity, the hydroxyl group of Ser-624 is more optimally positioned than that of Thr-623 for interacting with the chlorine of clofilium. Indeed, in some of the other models generated (i.e. not the lowest energy model) Thr-623 is not pointing into the cavity. The hydroxyl group on Thr-623 may only be in a position to interact with clofilium when Ser-624 is mutated. We propose that the chlorine atom of clofilium can interact with the polar hydroxyl group of either residue, but that a more specific high-affinity interaction occurs with Ser-624, possibly due to an optimal positioning of this residue. The sidechain of Val-625 is shielded from the inner cavity and therefore not implicated in binding any of the

16

compounds. Its sidechain performs an important packing role behind the selectivity filter. The V625A mutant has modified ion selectivity and inactivation properties, suggesting it affects drug binding indirectly.

The docking results suggest that increasing the length of the para-substituent – as in ibutilide and the amide analogue – prevents such molecules from adopting the same orientation as the nitro analogue (Figure 8B). The modelling results suggest that ibutilide can compensate for the increase in size by adopting an alternative favourable binding mode. In this configuration the methanesulphonamide (the para-substituent of ibutilide) also resides in the top corner of the cavity, suggestive of interactions with both Thr-623 and Ser-624. In this binding mode, an interaction is predicted between the sulphonyl group of ibutilide and the sidechain hydroxyl of Tyr-652. In addition, the phenyl ring of ibutilide is predicted to π-stack with another Tyr-652 in an edge-on-face interaction. A further hydrogen bond may also form between the hydroxyl group, one carbon away from the phenyl in ibutilide, and the sidechain of Ser-624 (Figure 8A). The amide analogue, lacking both the sulphonyl and hydroxyl groups of ibutilide, appears to be unable to adopt this orientation and interacts with neither Thr-623 nor Ser-624, with the nitrogen of its para-substituent binding centrally, at the intracellular mouth of the selectivity filter. The interactions with Tyr-652 are also limited (Figure 8B). This is consistent with the lower affinity of the amide analogue.

In all cases, the hydrophobic tail rests between all four Phe-656 residues (one from each subunit). Consistent with the finding that hydrophobicity, rather than aromaticity, of the residue at the position corresponding to Phe-656 was important for drug binding (Fernandez *et al*., 2004). A hydrophobic interaction may exist between the tail of the drug and a 'hydrophobic basket' formed at the base of the inner cavity by four Phe-656 residues and four Val-659 residues. Since the hydrophobic tail region of the compound does not change between quaternary and tertiary clofilium analogues, this explanation is supported by the identical shifts in affinity observed with F656A mutation between the two analogues.

There are a number of limitations to the study that should be taken into consideration. First, we measure current inhibition to investigate drug interactions, rather than measuring ligand binding directly. As mentioned previously, our measurements are influenced by factors such as membrane permeability that impact the free, intracellular concentration of drug. The potency of compounds in *Xenopus* oocytes is usually lower than in

17

mammalian cells; possibly because drug is absorbed by the yolk sack. Second, mutations of specific amino acids may alter drug block through an allosteric effect on the binding site. This is very likely to be the reason the V625A mutant reduces drug sensitivity. Third, structural differences within a compound series may alter drug properties such as lipophilicity and membrane permeability. We have minimized this by using very close analogues with CLogP values that differ by less than one log unit. Finally, we have used *in silico* docking studies to help visualize drug interactions and interpret our experimental findings. The modeling presented herein is based upon a closed state model of hERG. Current models are restricted by the lack of a crystal structure for hERG and because the dynamic conformational activities of the channel are not taken into account with the docking methods used. Nevertheless, the combination of mutagenesis, electrophysiological and computational techniques has proved valuable for understanding hERG channel block.

In summary, our results indicate that specific alterations in drug structure significantly altered the potency for block of WT-hERG channels. For instance, changing the para-substituent of clofilium analogues from polar to neutral reduced potency 100-fold. This was due to lower affinity interactions with pore (Thr-623 and Ser-625) and S6 (Tyr-652) helix residues. Molecular modelling provides an interpretation at the atomic level for the experimental data and further emphasizes the importance of pore helix residue interactions with the para-substituents of clofilium analogues. Our findings are likely to be applicable to many compounds and have important implications for the development of new drugs. Altering the para-substituent to reduce hERG binding could be highly beneficial if the efficacy against the primary target can also be maintained. Thus modifying the para-substituent could be a valuable strategy for reducing undesirable long QT side effects.

## References

Berman H. M., J. Westbrook, Z. Feng, G. Gilliland, T. N. Bhat, H. Weissig, I. N. Shindyalov, and P. E. Bourne (2000).. The Protein Data Bank. Nucleic Acids Res. 28 (1): 235-242.

Castle, N. A. (1991). Selective inhibition of potassium currents in rat ventricle by clofilium and its tertiary homolog. *Journal of Pharmacology and Experimental Therapeutics*, **257** (1): 342-50.

Cavalli, A., E. Poluzzi, F. De Ponti and M. Recanatini (2002). Toward a pharmacophore for drugs inducing the long QT syndrome: Insights from a CoMFA study of HERG K+ channel blockers. *Journal of Medicinal Chemistry*, **45** (18): 3844-3853.

Chen, J., G. Seebohm and M. C. Sanguinetti (2002). Position of aromatic residues in the S6 domain, not inactivation, dictates cisapride sensitivity of HERG and eag potassium channels. *Proc Natl Acad Sci USA*, **99** (19): 12461-12466.

DeLano, W.L. (2002) The PyMOL Molecular Graphics System 2002. http://www.pymol.org.

Doyle, D. A., J. Morais Cabral, R. A. Pfuetzner, A. Kuo, J. M. Gulbis, S. L. Cohen, B. T. Chait and R. MacKinnon (1998). The structure of the potassium channel: molecular basis of K+ conduction and selectivity. *Science*, **280** (5360): 69-77.

19

Ekins, S., W. J. Crumb, R. D. Sarazan, J. H. Wikel and S. A. Wrighton (2002). Three-dimensional quantitative structure-activity relationship for inhibition of human ether-a-go-go-related gene potassium channel. *Journal of Pharmacology and Experimental Therapeutics,* **301** (2): 427-34.

Fermini, B. and A. A. Fossa (2003). The impact of drug-induced QT interval prolongation on drug discovery and development. *Nature Reviews Drug Discovery*, **2** (6): 439-47.

Fernandez, D., A. Ghanta, G. W. Kauffman and M. C. Sanguinetti (2004). Physicochemical features of the HERG channel drug binding site. *Journal of Biological Chemistry*, **279** (11): 10120-7.

Ficker, E., W. Jarolimek, A.M. Brown (2001). Molecular determinants of inactivation and dofetilide block in ether a-go-go (EAG) channels and EAG-related K(+) channels. *Molecular Pharmacology*, **60** (6):1343-8.

Gessner, G. and S. H. Heinemann (2003). Inhibition of hEAG1 and hERG1 potassium channels by clofilium and its tertiary analogue LY97241. *British Journal of Pharmacology*, **138** (1): 161-71.

Gessner G., M. Zacharias, S. Bechstedt, R. Schonherr, S.H. Heinemann (2004). Molecular determinants for high-affinity block of human EAG potassium channels by antiarrhythmic agents. *Molecular Pharmacology*, **65** (5): 1120-9.

20

Herzberg, I.M., M.C. Trudeau, G.A. Robertson (1998). Transfer of rapid inactivation and sensitivity to the class III antiarrhythmic drug E-4031 from HERG to M-eag channels. *Journal of Physiology*, **511** (Pt 1):3-14.

Hille B. (1977). Local anesthetics: hydrophilic and hydrophobic pathways for the drug-receptor reaction. *Journal of General Physiology*, **69** (4):497-515.

Hondeghem L.M., B.G. Katzung (1977). Time- and voltage-dependent interactions of antiarrhythmic drugs with cardiac sodium channels. *Biochim Biophys Acta*, **472** (3-4): 373-98.

Jones, G., P. Willett, R.C. Glen, A.R. Leach, and R. Taylor (1997). Development and validation of a genetic algorithm for flexible docking. *Journal of Molecular Biology*, **267**: 727-48.

Kamiya, K., J. S. Mitcheson, K. Yasui, I. Kodama and M. C. Sanguinetti (2001). Open channel block of HERG K(+) channels by vesnarinone. *Molecular Pharmacology*, **60** (2): 244-53.

Keating, M. T. and M. C. Sanguinetti (2001). Molecular and cellular mechanisms of cardiac arrhythmias. *Cell*, **104** (4): 569-80.

Lees-Miller, J. P., Y. Duan, G. Q. Teng and H. J. Duff (2000). Molecular determinant of high-affinity dofetilide binding to HERG1 expressed in Xenopus oocytes: involvement of S6 sites. *Molecular Pharmacology*, **57** (2): 367-74.

21

Milnes JT, Crociani O, Arcangeli A, Hancox JC, Witchel HJ (2003). Blockade of HERG potassium currents by fluvoxamine: incomplete attenuation by S6 mutations at F656 or Y652. *Br J Pharmacol*. **139**(5):887-98.

Mitcheson, J. S., J. Chen and M. C. Sanguinetti (2000a). Trapping of a Methanesulfonanilide by Closure of the HERG Potassium Channel Activation Gate. *Journal of General Physiology*, **115** (3): 229-240.

Mitcheson, J. S., J. Chen, M. Lin, C. Culberson and M. C. Sanguinetti (2000b). A structural basis for drug-induced long QT syndrome. *Proc Natl Acad Sci USA*, **97** (22): 12329-12333.

Mitcheson, J. S. and M. D. Perry (2003). Molecular determinants of high-affinity drug binding to HERG channels. *Current Opinions in Drug Discovery and Development*, **6** (5): 667-74.

Pearlstein, R. A., R. J. Vaz, J. Kang, X. L. Chen, M. Preobrazhenskaya, A. E. Shchekotikhin, A. M. Korolev, L. N. Lysenkova, O. V. Miroshnikova, J. Hendrix and D. Rampe (2003). Characterization of HERG potassium channel inhibition using CoMSiA 3D QSAR and homology modeling approaches. *Bioorganic and Medicinal Chemistry Letters*, **13** (10): 1829-35.

Perry, M., M. J. de Groot, R. Helliwell, D. Leishman, M. Tristani-Firouzi, M. C. Sanguinetti and J. Mitcheson (2004). Structural determinants of HERG channel block by clofilium and ibutilide. *Molecular Pharmacology*, **66** (2): 240-9.

Recanatini, M., E. Poluzzi, M. Masetti, A. Cavalli and F. De Ponti (2004). QT prolongation through hERG K(+) channel blockade: Current knowledge and strategies for the early prediction during drug development. *Medicinal Research Reviews*, **25** (2): 133-66.

Sali, A. and T.L. Blundell (1993). Comparative protein modelling by satisfaction of spatial restraints. *Journal of Molecular Biology*, **234**: 779-815.

Ridley JM, Milnes JT, Witchel HJ, and Hancox JC (2004). High affinity HERG K(+) channel blockade by the antiarrhythmic agent dronedarone: resistance to mutations of the S6 residues Y652 and F656. *Biochem Biophys Res Commun,* **325**(3):883-91.

Sanchez-Chapula, J., R. A. Navarro-Polanco, C. Culberson, J. Chen and M. Sanguinetti (2002). Molecular determinants of voltage dependent HERG K+ channel block. *Journal of Biological Chemistry*, **277** (26): 23587-95.

Sanchez-Chapula, J. A., T. Ferrer, R. A. Navarro-Polanco and M. C. Sanguinetti (2003). Voltage-dependent profile of human ether-a-go-go-related gene channel block is influenced by a single residue in the S6 transmembrane domain. *Molecular Pharmacology*, **63** (5): 1051-8.

Sanguinetti, M. C., C. Jiang, M. E. Curran and M. T. Keating (1995). A mechanistic link between an inherited and an acquired cardiac arrhythmia: HERG encodes the IKr potassium channel. *Cell*, **81** (2): 299-307.

23

Sanguinetti MC, Mitcheson JS (2005). Predicting drug-hERG channel interactions that cause acquired long QT syndrome. *Trends in Pharmacological Sciences*, **26** (3):119-24.

Sanguinetti, M. C. and Q. P. Xu (1999). Mutations of the S4-S5 linker alter activation properties of HERG potassium channels expressed in Xenopus oocytes. *Journal of Physiology*, **514** ( Pt 3): 667-75.

Shealy, R. T., A. D. Murphy, R. Ramarathnam, E. Jakobsson and S. Subramaniam (2003). Sequence-function analysis of the K+-selective family of ion channels using a comprehensive alignment and the KcsA channel structure. *Biophysical Journal*, **84** (5): 2929-42.

Spector, P. S., M. E. Curran, M. T. Keating and M. C. Sanguinetti (1996). Class III antiarrhythmic drugs block HERG, a human cardiac delayed rectifier K+ channel. Open-channel block by methanesulfonanilides. *Circulation Research*, **78** (3): 499-503.

Steidl, J. V. and A. J. Yool (2001). Distinct mechanisms of block of Kv1.5 channels by tertiary and quaternary amine clofilium compounds. *Biophysical Journal*, **81** (5): 2606-13.

Suessbrich, H., R. Schonherr, S. H. Heinemann, F. Lang and A. E. Busch (1997). Specific block of cloned Herg channels by clofilium and its tertiary analog LY97241. *FEBS Letters*, **414** (2): 435-8.

Tseng, G. N. (2001). $I_{Kr}$: The hERG channel. *Journal of Molecular and Cellular Cardiology*, **33** (5): 835-849.

Vandenberg, J. I., B. D. Walker and T. J. Campbell (2001). HERG K+ channels: friend and foe.

*Trends in Pharmacological Sciences*, **22** (5): 240-6.

**Footnotes:**

This work was supported by grants to JSM from Pfizer Global Research and Development, UK, and the UK

Medical Research Council.

MOL #16741

**Figure Legends**

Figure 1. Comparison of WT-hERG block by clofilium and the tertiary compound PNU-0068611A.

*A*, Chemical structures of ibutilide, clofilium and PNU-0068611A. *B*, Outward currents (zero current shown by dashed line) recorded from WT-hERG expressed in *Xenopus* oocytes. Protocol duration was 6 s, with a 5 s depolarization to 0mV from a holding potential of –90 mV and peak tail current measured upon repolarization to –70 mV for 400 ms (*top*). Representative steady-state currents obtained following repetitive pulses before (control) and after addition of 300 nM clofilium (i) and 10, 30, 100 and 300 nM PNU-0068611A (ii). C, Concentration-response relationship for block of WT-hERG tail current by clofilium (■) and PNU-0068611A (▲). Mean $IC_{50}$ values are 80.84 ± 20.8 nM (n=6) for PNU-0068611A and estimated at ~30nM for clofilium. D, Comparison of time dependent block of WT-hERG by 10 µM clofilium (■) and PNU-0068611A (▲). Peak tail current measured after each test pulse to 0 mV in the presence of drug was normalised to the control current.

Figure 2. Concentration dependent block of pore helix mutant hERG channels expressed in *Xenopus* oocytes. *A*, Representative steady-state currents obtained from S624T(i) and S624A (ii) hERG channels following repetitive pulses before (control) and after the addition of increasing concentrations (as indicated) of PNU-0068611A. Note the significantly slowed deactivation observed with 3 µM PNU-0068611A, which may be due to recovery from block during the tail pulse to –70 mV. *B*, Concentration-response relationships for block of hERG channel currents by PNU-0068611A (*left*) and clofilium (*right*). $IC_{50}$ values are given in Table 3. *C*, Summary of fold changes in $IC_{50}$ values for each pore helix hERG mutant when compared to WT-hERG.

Figure 3. Rate of recovery from block of WT and S624A mutant hERG channels. *A & B*. Representative steady-state current traces from WT (A) and S624A mutant (B) hERG channels. Currents are shown prior to drug addition (control), following steady-state block by 10 µM PNU-0068611A, and 20 minutes after wash-out of the drug (WO). Note the greater recovery from block of S624A channels compared to WT-hERG. *C*. Mean time course for recovery from block of WT and S624A hERG by 10 µM PNU-0068611A (left) and clofilium (right).

27

Open symbols show steady-state block of tail currents from WT ($\square$) and S624A ($\triangle$) hERG. Closed symbols show mean peak tail currents during each repetitive pulse over a 20-minute period of wash-off. *D*. Summary of the fractional recovery from block after 20 minutes of drug wash-off. Calculated as $(I_{drug}-I_{wash-off})/(I_{control}-I_{drug})$.

Figure 4. Y652A and F656A mutations decrease affinity of hERG to clofilium and the tertiary compound PNU-0068611A. A, Concentration-response relationships for block of hERG tail currents by clofilium and PNU-0068611A. B, Summary of fold changes in $IC_{50}$ values for each S6 helix hERG mutant when compared to WT-hERG. $IC_{50}$ values are given in Table 3.

Figure 5. Altering the phenyl ring para-substituent significantly alters compound potency. *A to C*, Chemical structures of clofilium analogues (*top*). The analogues have a tertiary nitrogen and either nitro (*A*), amine (*B*), or amide (*C*) substituents at the para- position on the phenyl ring. Representative steady-state currents recorded from WT-hERG (*bottom*) are shown at a range of concentrations for each analogue. D, Concentration-response relationship for WT-hERG tail current block by tertiary clofilium analogues with either chlorine (PNU-0068611A, $\diamondsuit$), nitro (UK-062711-13, $\blacktriangle$), amine (UK-064962-01, $\blacksquare$), or amide (UK-064963-01, $\bigcirc$) at the para- position on the phenyl ring. $IC_{50}$ values are shown in Table 3.

Figure 6. Differential sensitivity of pore and S6 helix mutants to block by clofilium analogues. *A & B*, Mean concentration-response relationships for block of pore (*A*) and S6 (*B*) helix mutant channels by nitro, amine and amide clofilium analogues. Key to hERG channel subunits; $\blacklozenge$ WT, $\nabla$ T623A, $\blacksquare$ S624A, $\square$ S624T, $\bullet$ V625A, $\blacktriangle$ T623A:S624A, $\bigcirc$ F656A, $\blacktriangledown$ Y652A. Standard errors are not shown if bars are smaller than data symbol. $IC_{50}$ values are shown in Table 3. *C & D*, Fold changes in $IC_{50}$ values for each pore (*C*) and S6 (*D*) helix mutant relative to WT hERG.

Figure 7. Fold shifts in $IC_{50}$ induced by T623A:S624A and Y652A mutations, correlates well with compound potency in WT-hERG. *A & B*, For each clofilium analogue, fold shifts in $IC_{50}$ values (relative to WT-hERG)

induced by pore (*left*) and S6 (*right*) mutations are plotted against the corresponding WT-hERG IC$_{50}$ value. For T623A:S624A and Y652A there is a reasonable relationship between these values, suggesting these residues make an important contribution to binding interactions.

Figure 8. A cross-section through the hERG model, viewed perpendicular to the cell membrane, illustrating the predicted binding to the central cavity of hERG of (A) clofilium (yellow) and ibutilide (green), and (B) the nitro (green) and amide (yellow) clofilium analogues. The oxygen atoms of the hydroxyl groups of Thr-623 and Ser-624 are shown as spheres. Predicted hERG-ligand hydrogen bonds are depicted by black dashed lines. The hydrophobic tails of all four compounds are shown to interact with Phe-656, while the phenyl ring of all but the amide analogue is in a position to π-stack against Tyr-652. This predicted π-stacking interaction places the para-substituent in a suitable position to interact with hydroxyl sidechains of both Thr-623 and Ser-624. For clarity, only two of the four subunits of hERG are shown. In the case of ibutilide, the Tyr-652 residue that π-stacks with the drug is not depicted.
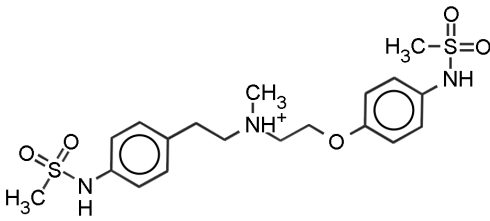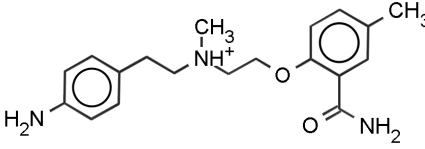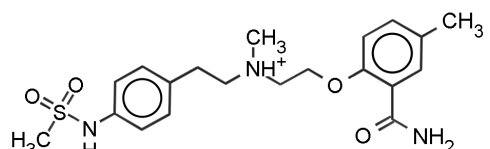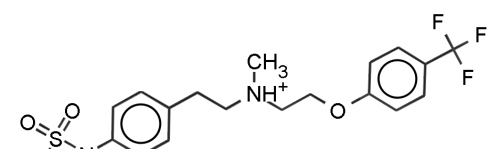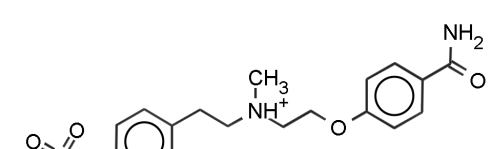
Table 1. Mean (± S.E.M.) activation and deactivation properties of hERG channel mutants.

Measurements were taken from current-voltage relationships . fitted with a Boltzman sigmoidal function to give the potential of half-maximal activation ($V_{0.5}$) and the slope of the activation curve. Time constants for fast ($\tau_{fast}$) and slow ($\tau_{slow}$) deactivation were obtained by fitting tail current decay at –70 mV with double exponential functions. * and ** indicate significance relative to WT hERG of P< 0.05 and 0.01 respectively. n ≥ 5 for all parameters..

| | Activation | | Deactivation | |
|---|---|---|---|---|
| | $V_{0.5}$ (mV) | k (mV). | $\tau_{fast}$ (ms) | $\tau_{slow}$ (ms) |
| Wild-type | -22.4 ± 1.5 | 8.2 ± 0.13 | 231 ± 5 | 1065 ± 32 |
| S624A | -24.2 ± 0.7 | 8.2 ± 0.28 | 391 ± 19** | 1549 ± 70** |
| S624T | -17.3 ± 0.8** | 8.1 ± 0.26 | 290 ± 13* | 1059 ± 71 |
| T623A | -24.2 ± 0.9 | 5.4 ± 0.18* | 208 ± 3** | 635 ± 63** |
| T623A:S624A | -23.4 ± 0.6 | 7.3 ± 0.15 | 183 ± 12** | 532 ± 32** |

Table 2. $IC_{50}$ values for WT-hERG tail current inhibition by dofetilide and four analogues that differ only in the

para-substituents.

| Compound | Structure | IC50 (nM) | n |
|---|---|---|---|
| Dofetilide | | 47.3 ± 4 | 8 |
| UK-068522 | | 2590 ± 280 | 7 |
| UK-068523 | | 81 ± 25 | 5 |
| UK-068526-01 | | 44 ± 6 | 7 |
| UK-068097 | | 922 ± 170 | 7 |

Table 3. IC$_{50}$ values for WT and mutant hERG current inhibition by four tertiary clofilium analogues with the indicated para-substituents on the phenyl ring. $\Delta$IC$_{50}$ represents the fold shift in IC$_{50}$ of each mutant channel compared to WT-hERG.

| Mutation | Nitro UK-062711-13 | | Amine UK-064962-01 | | Amide UK-064963-01 | | Chlorine PNU-0068611A | |
|---|---|---|---|---|---|---|---|---|
| | IC$_{50}$ (μM) | $\triangle$IC$_{50}$ | IC$_{50}$ (μM) | $\triangle$IC$_{50}$ | IC$_{50}$ (μM) | $\triangle$IC$_{50}$ | IC$_{50}$ (μM) | $\triangle$IC$_{50}$ |
| WT | 0.003 ± 0.05 | | 0.273 ± 0.02 | | 0.329 ± 0.09 | | 0.081 ± 0.02 | |
| T623A | 0.068 ± 0.01 | 27 | 9.284 ± 1.76 | 34 | 11.68 ± 3.18 | 36 | 0.845 ± 0.26 | 11 |
| S624A | 0.143 ± 0.02 | 57 | 8.206 ± 2.21 | 30 | 10.33 ± 1.33 | 32 | 2.263 ± 0.42 | 28 |
| S624T | 0.517 ± 0.10 | 207 | 2.958 ± 0.47 | 11 | 5.580 ± 0.68 | 17 | 1.117 ± 0.19 | 14 |
| T623A:S624A | 2.784 ± 0.29 | 1110 | 45.66 ± 2.14 | 167 | 9.380 ± 1.38 | 29 | 9.406 ± 1.80 | 116 |
| V625A | 1.481 ± 0.23 | 591 | 17.49 ± 2.80 | 64 | 13.57 ± 1.00 | 41 | 2.590 ± 0.22 | 32 |
| Y652A | 4.594 ± 0.56 | 1833 | 43.13 ± 6.27 | 158 | 42.64 ± 5.08 | 129 | 15.59 ± 1.30 | 193 |
| F656A | 6.738 ± 0.80 | 2688 | 115.1 ± 6.52 | 421 | 138.8 ± 12.5 | 422 | 33.96 ± 8.90 | 420 |
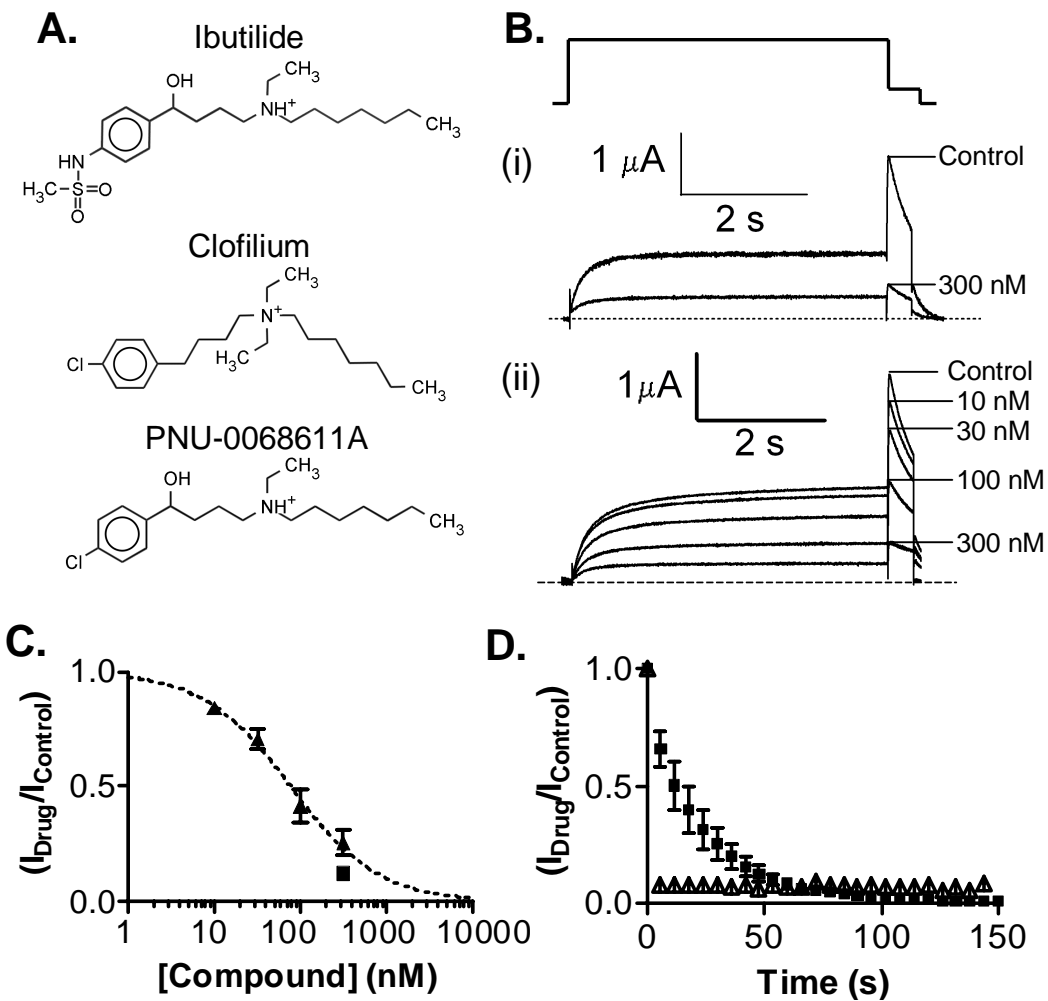
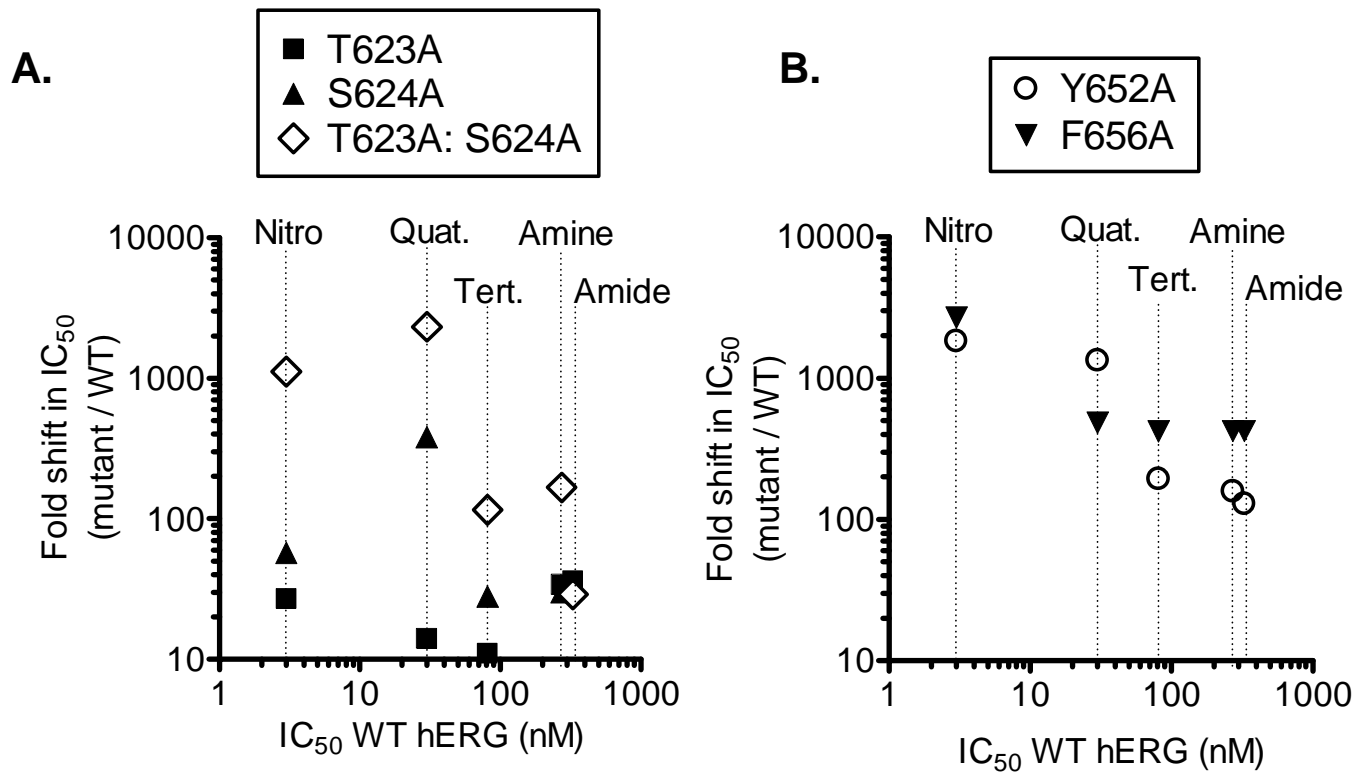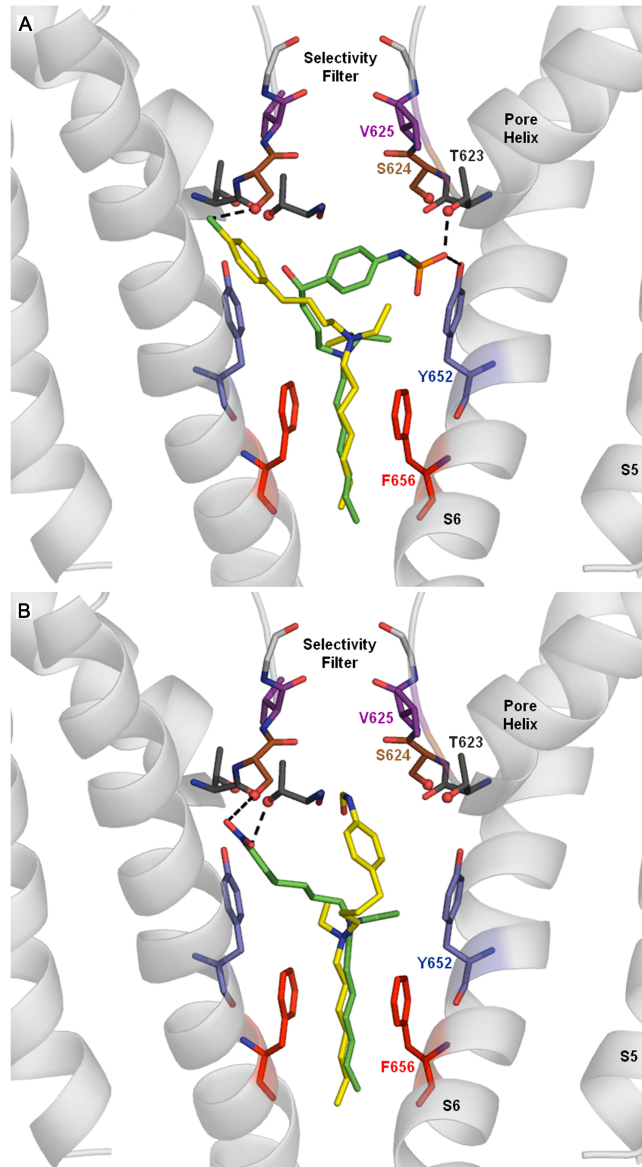Figure 1.

Figure 2

Figure 3.

**A.**



**B.**
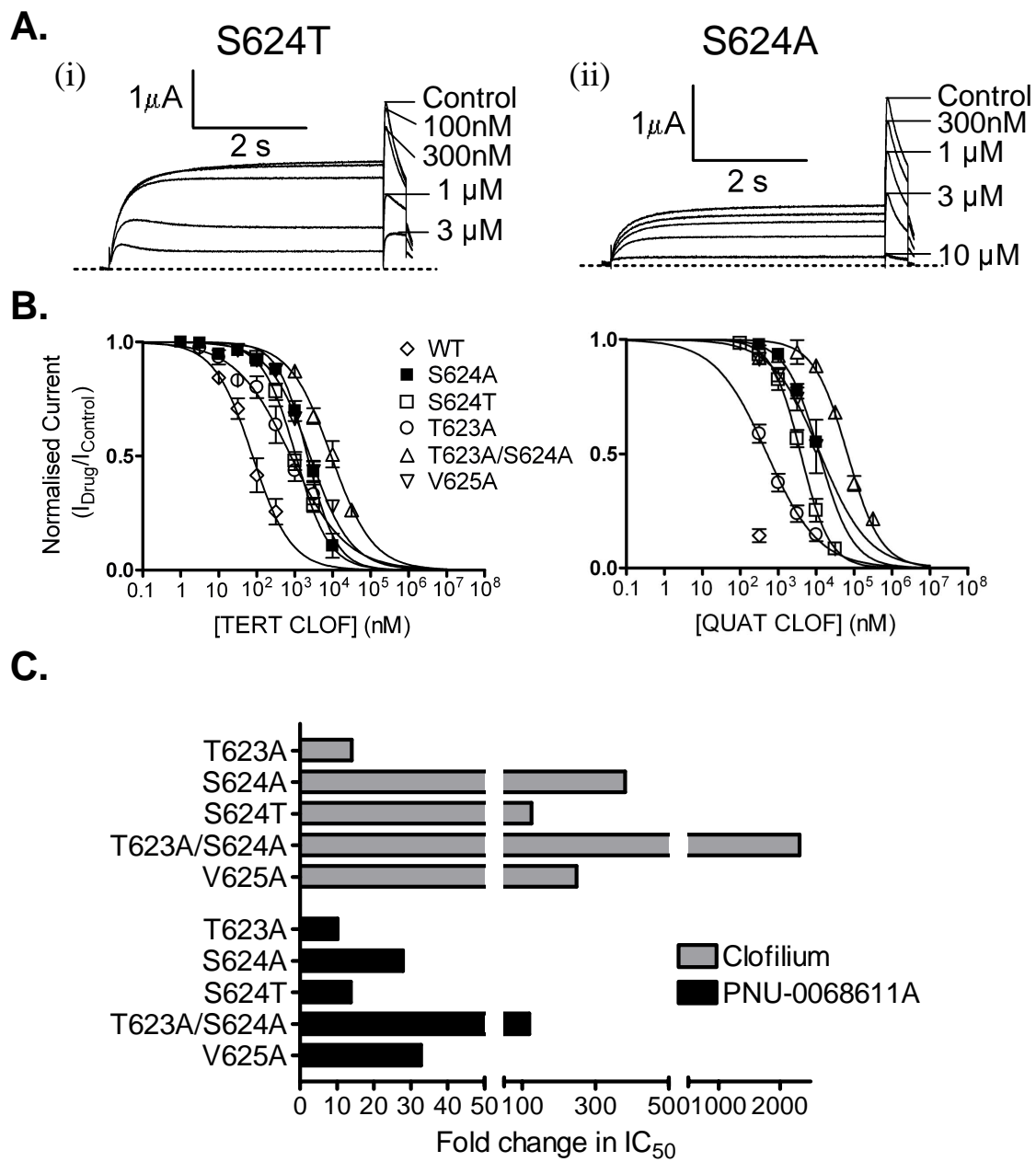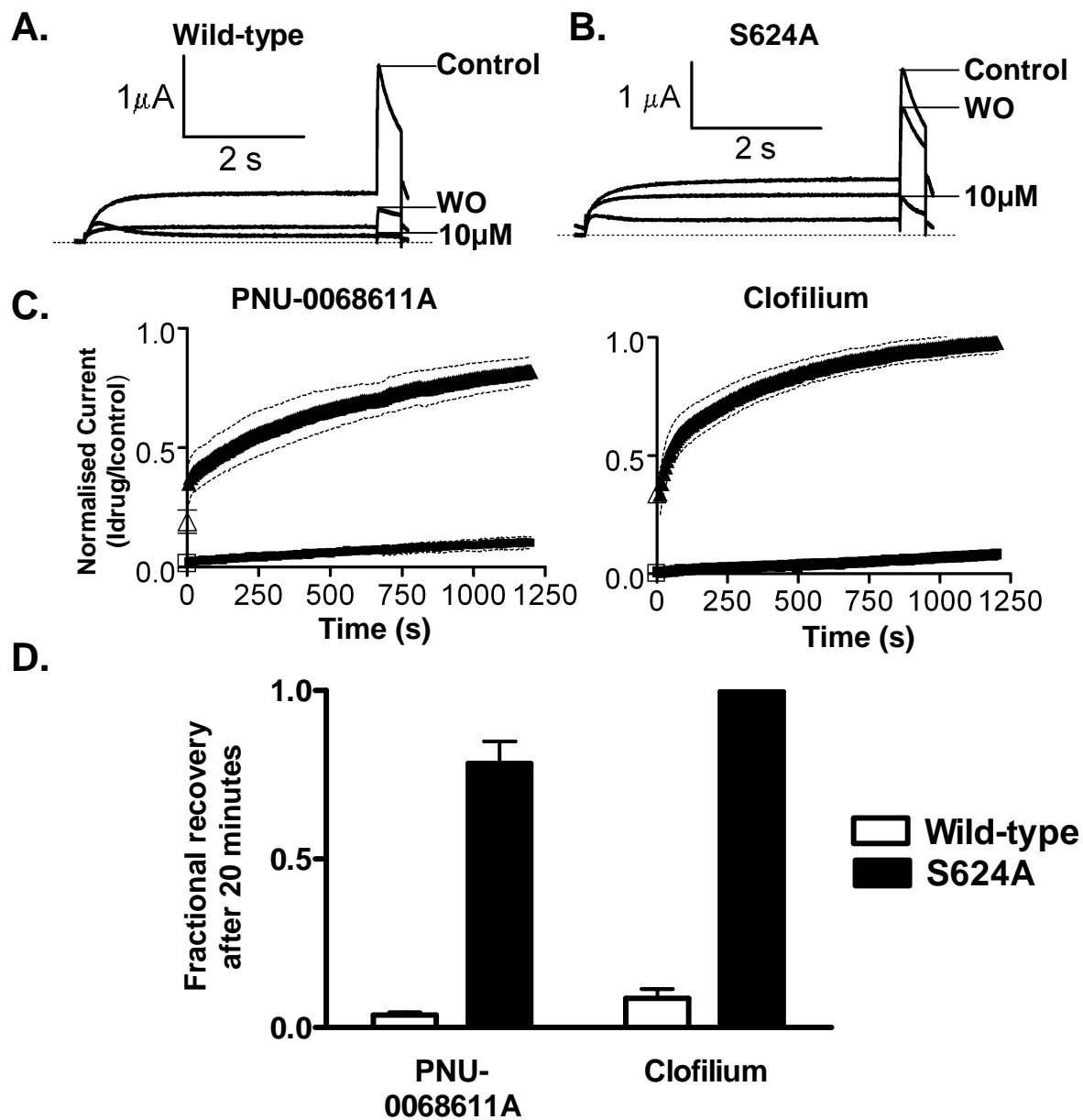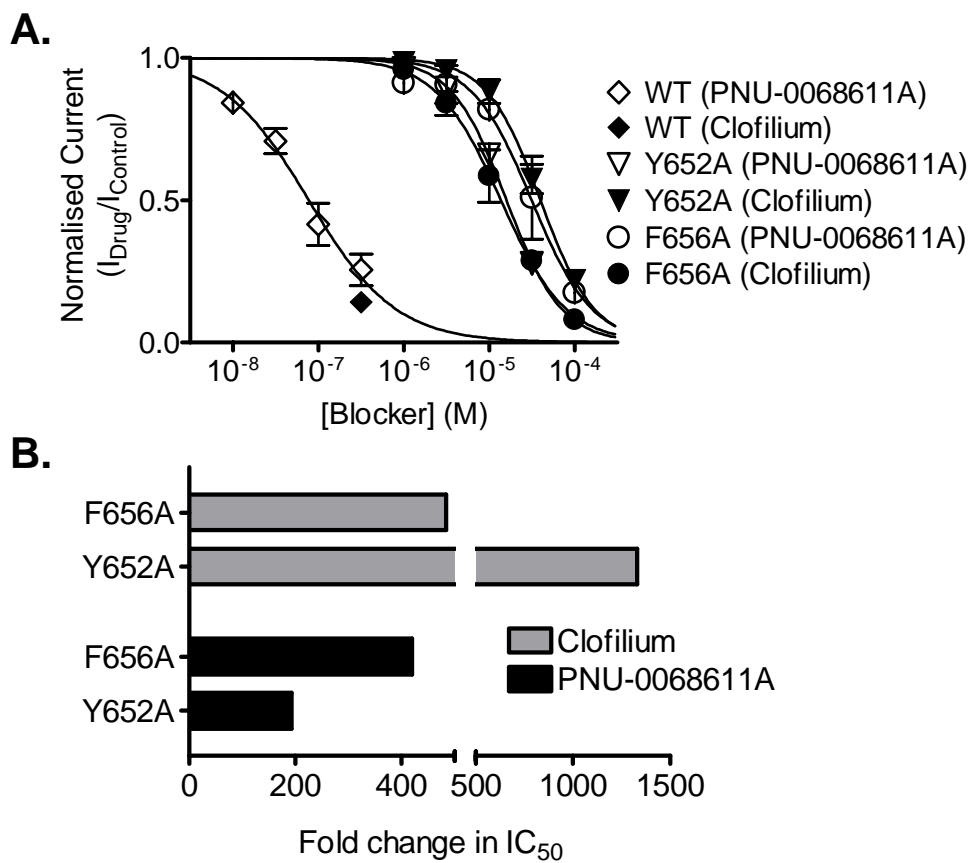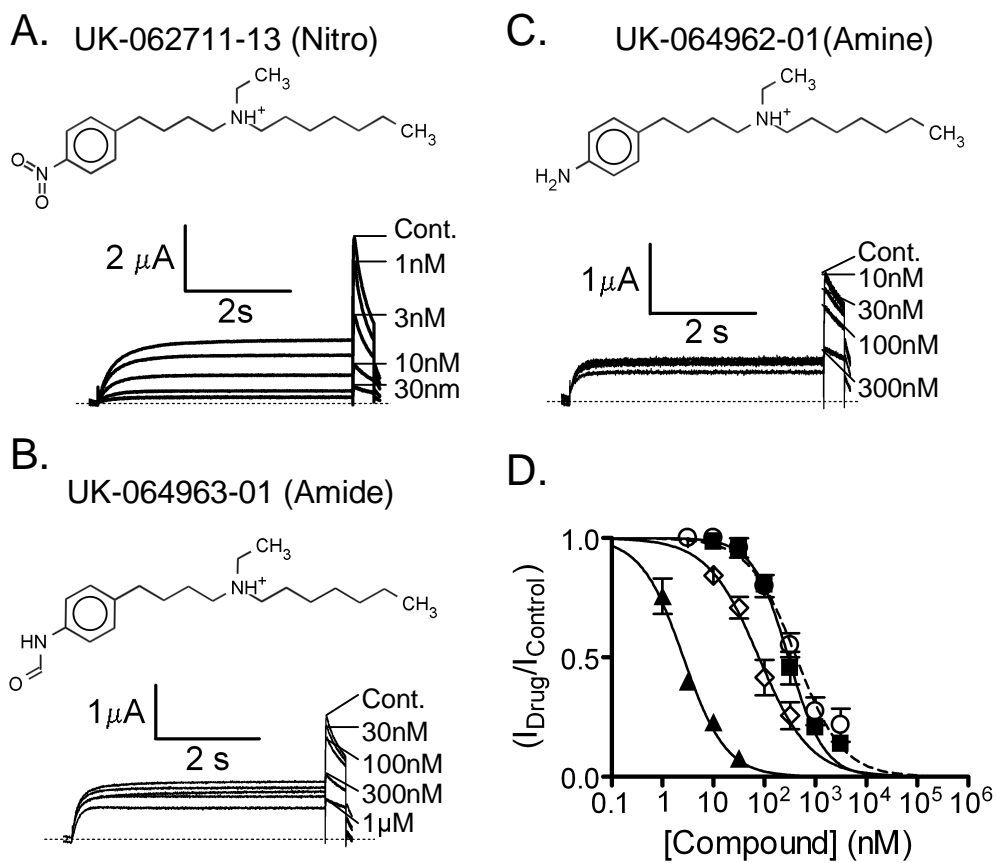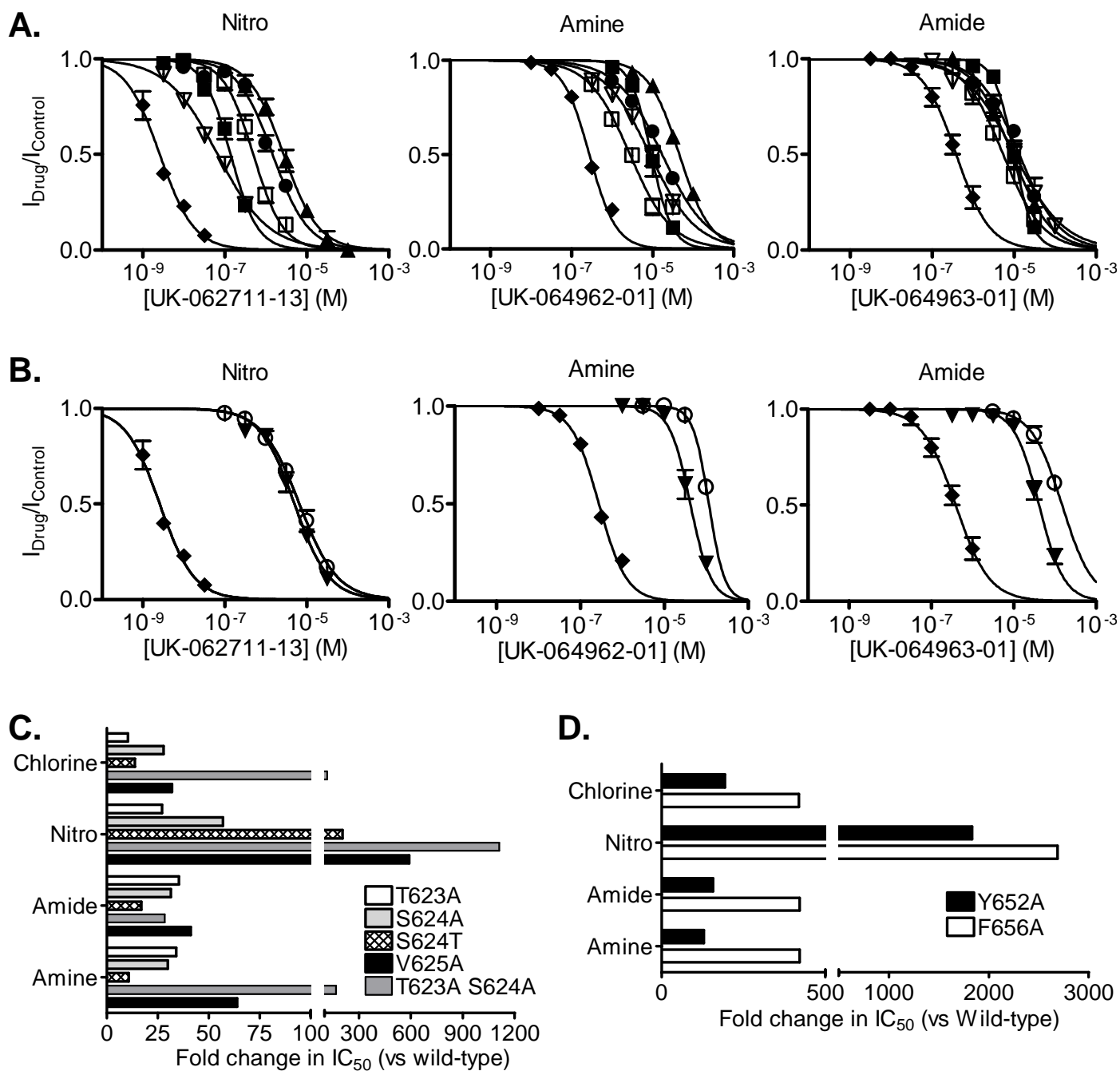


Figure 4.

Figure 5.

Figure 6.

Figure 7.

Figure 8